MATERIALE PLASTICE
https://revmaterialeplastice.ro
https://doi.org/10.37358/Mat.Plast.1964

Prediction of Optimal Parameter Settings and Significant Parameter for Reduced Geometric Deviations Through Multi Criteria Decision Making and Machine Learning Algorithms

SUBHASH SELVARAJ[1]*, RAJESH P. K.[2]
[1]Department of Mechanical Engineering, EASA College of Engineering and Technology, Coimbatore, 641105, India
[2]Department of Automobile Engineering, PSG College of Technology, Coimbatore, 641004, India

Abstract: *Part dimensional inaccuracies serve as a barrier from adopting Additive Manufacturing (AM) processes in mass production. Fused Deposition Modeling (FDM) is a thermoplastic based low cost AM process which can create conceptual models, prototypes and end user industrial parts. The current study involves predicting the optimal parameter settings and significant parameter for reduced geometric deviations in printed part using Nylon filament reinforced with 20% carbon fiber. Five input factors such as build orientation, layer thickness, infill density, raster angle and infill pattern have been considered for preparing the experimental layout through taguchi's mixed fractional factorial design. The changes in length, width and thickness of the printed part from CAD value have been evaluated individually through ANOVA and Signal to Noise Ratio method (Smaller the better). Layer thickness is significant only for variations in length, but build orientation affects both width and thickness dimensions. The geometric deviations are further analyzed using combined multi criteria decision making (MCDM) approaches such as Entropy-CoCoSo and PCA-TOPSIS. The optimal parameter settings obtained for reduced geometric deviations is found to be Flat orientation, 0.1mm layer thickness, 50% infill density, 0° raster angle and cubic infill pattern. Layer thickness is found to be highly significant parameter influencing the geometric deviations subsequently followed by build orientation from both the MCDM methods. The multi response performance index values obtained from Entropy-CoCoSo has been trained using classification algorithms such as decision tree, random forest and Naïve Bayes. Naïve Bayes algorithm outperformed other methods with highest classification accuracy of 99.4% in a training-testing split ratio of 75:25.*

Keywords: *nylon composites, Principal Component Analysis, TOPSIS, CoCoSo, entropy, decision Tree Algorithms*

1. Introduction

Manufacturing industries have undergone a massive shift in way of producing components from traditional means. Manufacturing industries apply physical or chemical processes for attaining the desired changes or transformations in raw materials with the involvement of machineries, technologies and skilled manpower. Industry 4.0 is a current trend in manufacturing, where production is carried out using highly automated technologies that provide more exact quality control, faster time to market, and less complexity [1]. Additive manufacturing (AM) or 3D printing can be defined as any process which creates parts from CAD file by adding layers one over another with fascinating benefits such as less waste, zero tooling and instant response to any shape formation [2]. Fused Deposition Modeling (FDM) is one such AM process which falls under material extrusion technique where the initial material in the form of thin wire or filament extruded through a heated nozzle to deposit layers of material one over another to create the final part [3]. FDM process involves numerous parameters which can be categorized as material specific, machine specific and operation specific which has significant impact over the part produced as an individual or in combination with other parameter. FDM process is continuously expanding its material library due to its potential in creating parts at low cost and less complexity.

email: subhashraj18@gmail.com

Metals, ceramics, polymers and their composites can be used as feedstock in FDM machine for conceptual models, functional prototypes and end use industrial parts. ABS and PLA are the most widely adopted materials used in FDM process due to their flexibility to undergo the process at low operating conditions [4]. Due to their beneficial qualities, like being light in weight, flexible, self-lubricating, and having excellent resistance to chemical environments, polymers are widely used in a variety of sectors. Despite the fact that polymers like plastic pose a serious threat to the environment, industrial products are still being developed using this material because of its unbeatable advantages. Polymer matrix composites have proven to be a viable option for many industrial applications, including those in automotive, packaging, aerospace, and the field of medicine. Owing to the disadvantages associated with FDM parts such as poor mechanical properties, high surface roughness and dimensional inaccuracies, porous structure, optimization of FDM process parameters are highly essential to produce parts matching the demand of industrial scenario. Ji-man et.al [5] evaluated the dimensional accuracy of 3D printed dental casts printed by different techniques such as FDM, SLA, DLP and Polyjet. The authors have reported that the dimensional accuracy of FDM printed dental cast is inferior and it has undergone contraction at cylindrical locations. Radomir et.al [6] investigated the effect of FDM process parameters over surface roughness and dimensional accuracy of PLA thermoplastic. Both the output responses are severely affected by layer height. Prairit et.al [7] predicted the dimensional accuracy of FDM parts printed using ABS and PLA material through response surface methodology coupled with supervised machine learning algorithms. The overall average percentage deviation is around 6% and ABS parts has significant lower deviations than PLA. Dimensional and surface texture characterization of ABS-plus material have been carried out by Nunez et.al [8] by varying layer thickness and infill density. Low dimensional error is resulted from 0.178 mm layer thickness and 100% infill density. Noriega et.al [9] adopted artificial neural network for reducing the dimensional error and they have recommended that ANN has the capability to predict the accuracy of dimensional error with low error percentage. Rupinder and Alok [10] employed barrel finishing process for reducing the surface roughness and dimensional deviations by varying five different parameters for shapes such as rhomboid and cube shaped FDM parts. The post processing of FDM parts through barrel finishing process has reduced the stair stepping effect with low dimensional deviations to an acceptable level. Nathan and Albert [11] proposed a simplified benchmarking model for with part features such as rectangular boss, rectangular void, cylindrical boss and a cylindrical void. For assessing the dimensional accuracy of FDM parts. The proposed model is found to have better performance than the models proposed in the past studies. The dimensional accuracy of aluminium matrix composite using taguchi L_9 orthogonal array is performed by Rupinder singh et.al [12] by incorporating nylon-6 waste based reinforced filament. Taguchi based optimization of parameter settings have reduced the dimensional error by 1.49%.Chohan et.al [13] employed statistically controlled vapor smoothing process for enhancing the dimensional accuracy of FDM printed biomedical implants and they have reported that the post processing technique has shown appreciable improvements in dimensional accuracy. The analysis and optimization of dimensional accuracy, porosity for high impact polystyrene material through evolutionary algorithms has been performed by Manjunath et.al [14]. The optimal process conditions obtained has recommended for low layer thickness and 100% infill density for reduced dimensional error and porosity formation. Both Bald eagle search and Rao 3 algorithms are computationally efficient for attaining global solutions. Sherri et.al [15] discussed the effect of raster angle and build orientation over dimensional error for eleven different materials. The information shared by the authors serve as a good resource for understanding the effect of FDM parameters over dimensional accuracy for different materials.

The application of designed experiments and computational algorithms for obtaining the optimal process settings for enhancing the mechanical properties and reducing the process shortcomings such as surface roughness, dimensional error and porosity are widespread [16, 17]. Methods such as multi criteria decision making are found to be efficient in identifying the optimal conditions towards combined objectives in many research problems. Phaneendra et.al [18] combined taguchi and grey relational analysis for optimizing the mechanical properties of E-glass/polyester composites. Sudhagaret.al [19]

adopted both TOPSIS and grey relational analysis for improving the process outputs from friction stir welding process for aluminium 2024 alloy. The optimal conditions arrived from both the methods are found to be same. Pooja et.al [20] optimized FDM process parameters for PLA material using grey relational analysis and optimal conditions has shown an improvement of 10.10% bin grey relational grade compared with initial settings.

Machine Learning (ML) algorithms have grabbed the attention of researchers due to their potential in arriving the feasible solution at lesser time with greater accuracy. The adoption of ML algorithms in FDM parameter optimization has been witnessed recently. Vijaykumar et.al [21] optimized FDM process parameters using desirability approach and machine learning regressor for PLA material. The models developed by both the methods are able to predict tensile, impact and flexural strength with low error percentage. Juan et.al [22] predicted surface roughness of FDM parts using decision tree methods for PETG material. Random forest algorithm performed better in prediction of surface roughness than other methods such as C4.5 and random tree algorithms.

In addition, dimensional error studies have been combined with other part characteristics such as surface roughness by many authors. Prithu et.al [23] combined both dimensional error and surface roughness n their study to optimize the FDM process parameters for PET-G parts. The authors have varied four different FDM parameters such as layer thickness, print speed, extrusion temperature and raster width with five levels through central composite design. The sample printed for evaluation consists flat, inclined and curved surfaces for measuring surface roughness and dimensional error. The errors measured have been further analyzed for development of mathematical models. ANFIS have been employed to test and train the experimental outcomes to predict them for new set of process parameters. The validation carried out ensures the potential of ANFIS in predicting the experimental outcomes with less error. Nagendra et.al [24] printed tensile tests specimens and evaluated the dimensional accuracy of the polycarbonate samples through taguchi orthogonal array and calculated the international tolerance grade for the dimensions involved. The optimum parameter combination for the linear and radial dimension observed are found to be similar in terms of layer thickness and part orientation with 0.1 mm and flat positioned part printing, but it differs in case of raster angle which stimulated the need of multi objective optimization of process parameters. The calculated IT grades have shown that linear dimension has lower IT grade than radial dimension. Aslani et.al [25] employed techniques such as grey relational grade, analysis of variance and analysis of means for analyzing the dimensional accuracy of part printed using PLA. The authors have printed parts with two different set of parameter combinations and the second phase setting (optimized parameter setting) is found to possess better dimensional accuracy than the first one.

There are many application of the carbon nylon filaments in manufacturing industry for tooling, functional prototypes, sporting goods, drones which are useful in the fields of automotive, aerospace, robotics where the parts require to have high mechanical properties such as strength, stiffness, maintain dimensional stability, rigidity, durability etc.

The literature survey carried out unveils the inability of FDM process to create parts with good dimensional accuracy. The current study considers five different FDM parameters such as layer thickness, build orientation, infill density, raster angle and infill pattern varying in different levels as per L18 mixed fractional factorial design using Minitab 17.0. The sample for the study has been prepared in accordance with Shore D hardness ASTM D2240 standard to ascertain the dimensional inaccuracies resulting in the printed part using Nylon 6/66 copolymer filament reinforced with 20% carbon fiber. The prepared samples are checked for dimensional accuracy by checking the sample's length, width and thickness using digital vernier caliper. The experimental values is further analyzed using combined approach of Entropy – CoCoSo and PCA-TOPSIS methodologies for identifying the optimal parameter settings which can reduce the dimensional inaccuracies. The multi response performance index resulting from the combination of different methods have been analyzed using ANOVA to find the significant factor affecting the output responses and its crucial contribution among the input parameters considered. The MRPI values are further trained and tested using machine learning algorithms to correlate the

optimal parameter settings obtained from MCDM method. The proposed research methodology has been depicted in the form of flow chart at Figure 1.

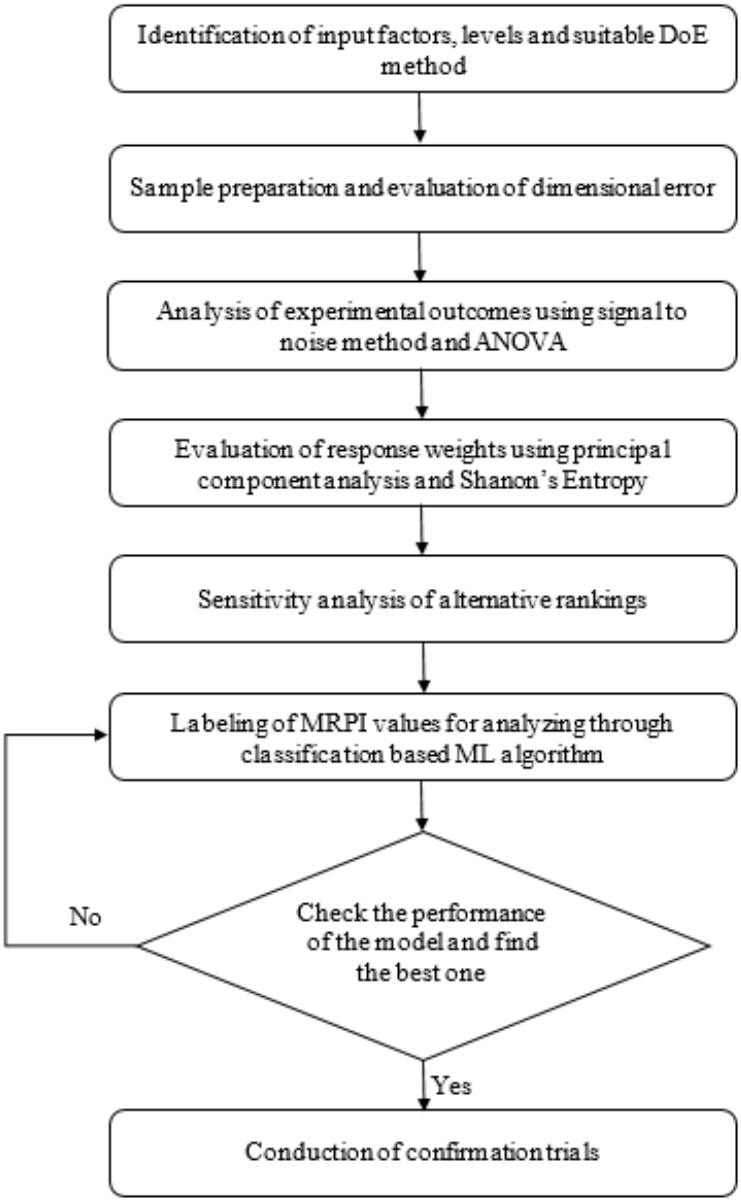

Figure 1. Proposed Research Methodology

2. Materials and methods

The current section details about the filament material and FDM printer adopted for preparing sample. The section also highlights about the technique behind the experimental layout followed in making the samples.

2.1. Filament material

The filament material for the study was supplied by eSun, China with nylon 6/66 copolymer as the matrix phase and 20% carbon fiber as the reinforcing material. The addition of carbon fiber greatly increases the strength, rigidity and toughness of nylon, and can replace metal materials in many occasions. Self-lubricating wear resistance makes this carbon fiber 3d printer filament suitable for printing gears. It has high dimensional stability, excellent printability and superior abrasive resistance.

The filament is of 1.75mm diameter and black colored. Table 1 represents various properties of nylon carbon fiber filament.

Table 1. Various Properties of Filament Material

S.No	Parameter / Characteristic	S.I Unit	Value
1	Density	g/m^3	1.24
2	Melt flow index	g/10 min	11.46
3	Tensile Strength	MPa	140
4	Elongation at break	%	10.61
5	Flexural Modulus	MPa	4363
6	Izod impact strength	kJ/m^2	18.67
7	Extruder Temperature	ºC	260-300
8	Bed temperature	ºC	45-60
9	Printing Speed	mm/s	40-100

2.2. FDM printer

Flash forge Creator 3 Pro, a professional FDM printer made from china has been used for sample preparation in the current study and shown in Figure 2. The machine comprises dual extruder which can extrude filaments through the heated nozzle with maximum extrusion temperature of 320 ºC. The machine has a build volume of 300x250x200 mm which is in good accordance with the dimensions of almost all ISO and ASTM standard testing samples. The machine supports multi-mode printing and flexible heated bed supports for the easy removal of printed part from the machine. The machine has good compatibility for printing materials such as PLA / ABS / PA / PC / PVA / HIPS / PETG / Wood / ASA and their fiber reinforced composite filaments. Extrusion nozzles with varying materials such as stainless steel and carbon steel can be used with optional diameters such as 0.4, 0.6 and 0.8mm. CURA slicing software is adopted for slicing the 3D model in to thin layers and variation of other input factors.

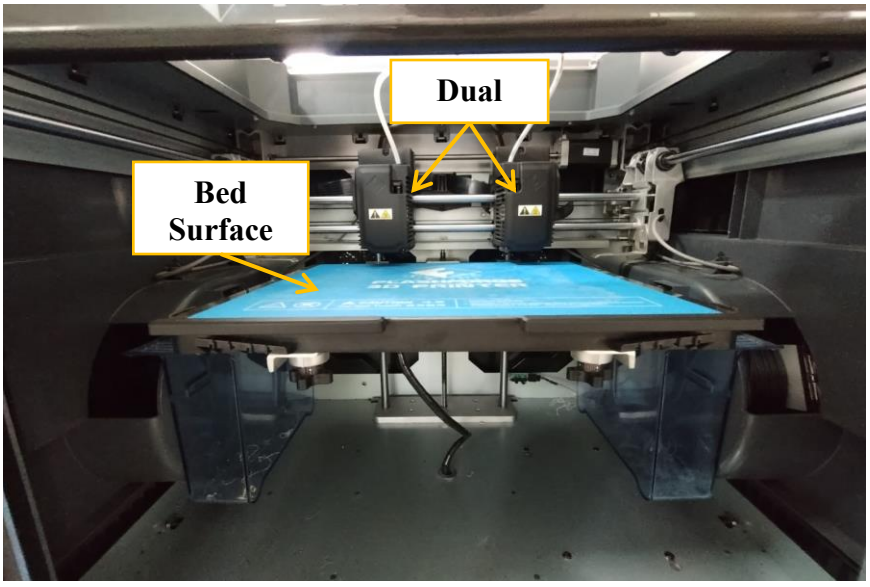

Figure 2. Flash forge Creator 3 Pro FDM Printer

2.3. Design of Experiments

Designed experiments play a pivotal role in experimental research as it provides highly accurate results at lesser number of experiments and low cost. Taguchi's orthogonal array can be used for designing experimental trials by varying input parameters to desired levels for conducting experiments. The current study considers mixed level fractional factorial design by varying five different input parameters such as build orientation, layer thickness, infill density, raster angle and infill pattern as shown in Table 2. The current study varies build orientation with two levels and all other four parameters are varied with three levels. A total of 18 experimental trials have been created by mixing the input parameters of different levels using Minitab 17.0 software. Table 3 shows the experimental design matrix in uncoded units for sample preparation.

Table 2. FDM Input Parameters and their Levels

Input Parameter	Symbol	S.I Unit	Level 1	Level 2	Level 3
Build Orientation	A	-	Flat	On edge	-
Layer Thickness	B	mm	0.10	0.17	0.24
Infill Density	C	%	50	75	100
Raster Angle	D	°	0	45	90
Infill Pattern	E	-	Cubic	Triangles	Grid

Table 3. Taguchi L_{18} Experimental Layout with Input factors in uncoded units

Trial No	A	B (mm)	C (%)	D (°)	E
1	Flat	0.1	50	0	Cubic
2	Flat	0.1	75	45	Triangles
3	Flat	0.1	100	90	Grid
4	Flat	0.17	50	0	Triangles
5	Flat	0.17	75	45	Grid
6	Flat	0.17	100	90	Cubic
7	Flat	0.24	50	45	Cubic
8	Flat	0.24	75	90	Triangles
9	Flat	0.24	100	0	Grid
10	On edge	0.1	50	90	Grid
11	On edge	0.1	75	0	Cubic
12	On edge	0.1	100	45	Triangles
13	On edge	0.17	50	45	Grid
14	On edge	0.17	75	90	Cubic
15	On edge	0.17	100	0	Triangles
16	On edge	0.24	50	90	Triangles
17	On edge	0.24	75	0	Grid
18	On edge	0.24	100	45	Cubic

Experimental work

The current study involves measuring the geometric deviations arising in samples prepared through FDM process by varying five different input parameters. The sample has been prepared with dimensions 25 x 20 x 6.4 mm (Length x Width x Thickness respectively) which has good accordance with ASTM 2240 shore D hardness measurement sample. The prepared samples have been measured for deviations in dimensions with reference to the CAD design value by using a digital vernier caliper by taking each measurement thrice and the average value have been tabulated for further observation. Figure 3 shows the 18 different samples printed as per taguchi's L18 orthogonal array by combining different input parameters. The varying infill patterns considered for the samples such as cubic, triangular and grid is depicted in Figure 4.

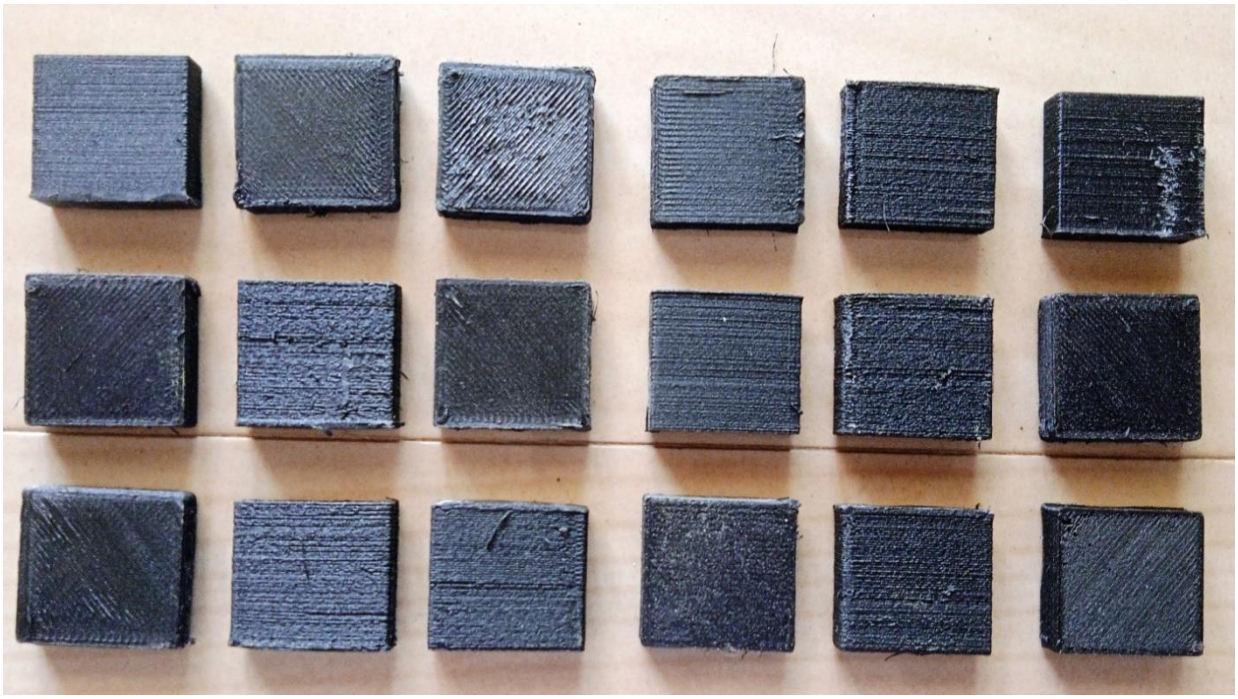

Figure 3. Hardness Specimen as per ASTM 256 Standard

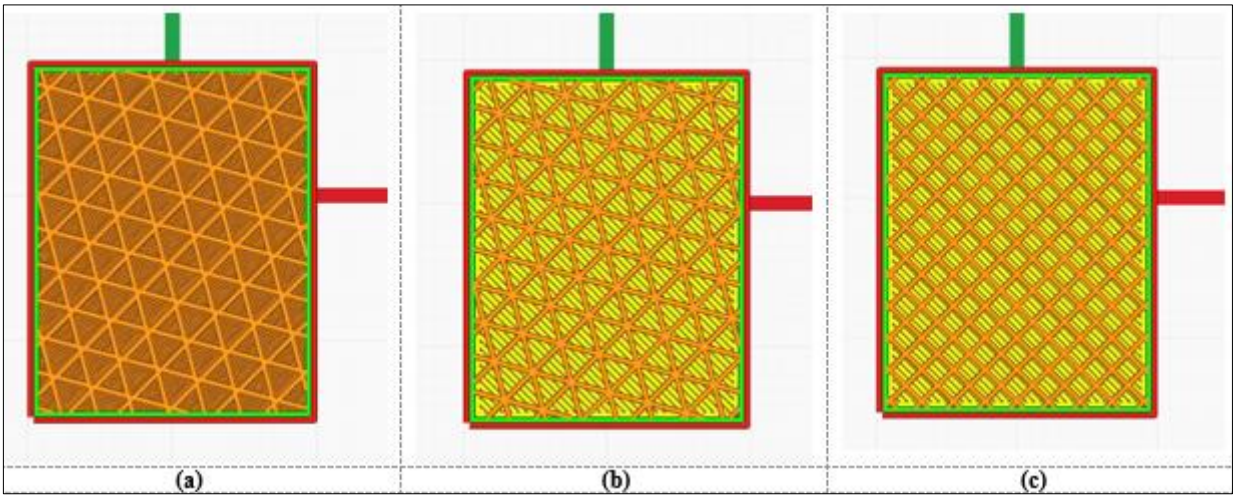

Figure 4. Infill Patterns (a) Cubic (b) Triangular (c) Grid

Table 4. Measured Values and Geometric Deviations of Experimental Samples

Trial No	A	B (mm)	C (%)	D (°)	E	Measured values			Geometric Deviations		
						L (mm)	W (mm)	T (mm)	ΔL (mm)	ΔW (mm)	ΔT (mm)
1	1	1	1	1	1	25.23	20.07	6.46	0.23	0.07	0.06
2	1	1	2	2	2	25.42	20.43	6.42	0.42	0.43	0.02
3	1	1	3	3	3	25.45	20.56	6.42	0.45	0.56	0.02
4	1	2	1	1	2	25.67	20.74	6.39	0.67	0.74	-0.01
5	1	2	2	2	3	25.62	20.63	6.20	0.62	0.63	-0.20
6	1	2	3	3	1	25.68	20.92	6.45	0.68	0.92	0.05
7	1	3	1	2	1	25.43	20.49	6.39	0.43	0.49	-0.01
8	1	3	2	3	2	25.89	20.99	6.39	0.89	0.99	-0.01
9	1	3	3	1	3	25.68	20.79	6.58	0.68	0.79	0.18
10	2	1	1	3	3	25.05	19.80	6.75	0.05	-0.20	0.35
11	2	1	2	1	1	25.08	19.74	6.59	0.08	-0.26	0.19
12	2	1	3	2	2	25.27	19.75	6.80	0.27	-0.25	0.40
13	2	2	1	2	3	25.44	19.82	7.23	0.44	-0.18	0.83
14	2	2	2	3	1	25.25	19.83	6.88	0.25	-0.17	0.48
15	2	2	3	1	2	25.66	19.73	7.27	0.66	-0.27	0.87
16	2	3	1	3	2	25.39	19.87	7.11	0.39	-0.13	0.71
17	2	3	2	1	3	25.50	19.67	6.98	0.50	-0.33	0.58
18	2	3	3	2	1	25.61	19.76	7.24	0.61	-0.24	0.84

The measured values of sample dimensions have been tabulated and observed. The geometric deviations recorded in sample length are positive in nature and the maximum deviation of 0.89mm is observed when the layer thickness is maximum at flat orientation. The deviations observed are not within the tolerance limit of the process ± 0.1mm. At high layer thickness, stair stepping effect will be higher and the minimum deviation of 0.05mm is resulted from on edge orientation with lower layer thickness. The deviation in width direction is of mixed nature where flat oriented samples have resulted with positive deviations and on edge oriented samples have exhibited negative deviations. The deviation follows a growing trend when there is an increase in layer thickness in combination with infill density. The thickness deviations have both positive and negative values in both the orientations. This is due to the fact that the sample undergoes heating and cooling during layer deposition which generally leads to sample warping.

The deviations observed are primarily due to the effect of alternating heating and cooling cycles of the process which leads to shrinkage. At higher infill density such as 100 %, the samples get filled completely and it induces expansion to the sample when cooling down to room temperature from extrusion temperature. The negative deviation of the sample is observed primarily in both width and thickness directions. The negative deviation was above the tolerance limit in case of width direction when the on-edge orientation was considered. But in terms of thickness direction, flat orientation has produced negative deviations and most of them are within the tolerance limit.

The experimental values are further analyzed using ANOVA with a confidence interval of 95% with $p \leq 0.05$ and the results have been observed for significant and insignificant parameter with p value $\leq$ 0.05.

Table 5. ANOVA Results for ΔL (mm)

Source	DoF	Adj SS	Adj MS	F-Value	P-Value	Contribution %
A	1	0.184022	0.184022	18.3	0.003	21.18
B	2	0.408044	0.204022	20.29	0.001	46.96
C	2	0.108344	0.054172	5.39	0.033	12.47
D	2	0.001078	0.000539	0.05	0.948	0.12
F	2	0.086978	0.043489	4.32	0.053	10.01
Error	8	0.080444	0.010056	---	---	9.26
Total	17	0.868911	---	---	---	100

Table 6. ANOVA Results for ΔW (mm)

Source	DoF	Adj SS	Adj MS	F-Value	P-Value	Contribution %
A	1	0.72802	0.72802	22.07	0.002	52.53
B	2	0.16030	0.08015	2.43	0.150	11.57
C	2	0.13843	0.06922	2.10	0.185	9.99
D	2	0.04990	0.02495	0.76	0.500	3.60
F	2	0.04530	0.02265	0.69	0.531	3.27
Error	8	0.26384	0.03298	---	---	19.04
Total	17	1.38580	---	---	---	100

Table 7. ANOVA Results for ΔT (mm)

Source	DF	Adj SS	Adj MS	F-Value	P-Value	Contribution %
A	1	1.22201	1.22201	50.89	0.000	70.02
B	2	0.20201	0.10101	4.21	0.056	11.58
C	2	0.06481	0.03241	1.35	0.313	3.71
D	2	0.03908	0.01954	0.81	0.477	2.24
F	2	0.02514	0.01257	0.52	0.611	1.44
Error	8	0.19211	0.02401	---	---	11.01
Total	17	1.74516	---	---	---	100

The results of ANOVA indicates that layer thickness is the dominant factor influencing the geometric deviations in length with crucial contribution of 46.96%, followed by build orientation with 21.18 % and infill density has 12.47% contribution. In case of width variations, build orientation ranks top with 52.53 and no other factor is found to be significant. For thickness deviations build orientation is the significant parameter with 70.02% followed by layer thickness with 11.58%. Table 5, 6 and 7 shows the ANOVA results for observed geometric deviations. Table 8 shows the model summary of all the three output responses and the value of R-square is more than 80% for all the three output responses which ensures the model significance. Table 8 shows the model summary for all the three output responses. The maximum error percentage resulted from ANOVA analysis is found to be 19.04 which is in the acceptable range.

Table 8. Model Summary for Output Responses

Output Parameter	S	R-sq	R-sq (adj)	R-sq (pred)
ΔL (mm)	0.10028	90.74%	80.33%	53.13%
ΔW (mm)	0.18161	80.96%	59.54%	3.61%
ΔT (mm)	0.15496	88.99%	76.61%	44.27%

The main effect plot generated through Minitab 17.0 software highlights the optimal combination for attaining the reduced dimensional inaccuracy for the output responses and response table highlights the significant parameter influencing the output responses. Table 9 represents the optimal parameter combination and significant input parameter affecting the output response.

Table 9. Summary of Optimal parameter Combination and Significant Input parameter

Output Parameter	Optimal Combination	Significant Parameter
ΔL (mm)	A2B1C1D3E1	Layer Thickness
ΔW (mm)	A2B1C1D1E1	Build Orientation
ΔT (mm)	A2B1C1D3E2	Build Orientation

The significant parameter recommended by response table and ANOVA results are in good accordance. The optimal parameter conditions obtained are found to be different for all the three output responses measured and this stimulates the need of conducting multi response optimization of output responses through standard procedures.

Multi Objective Optimization

Multi objective optimization transforms every individual objective in to a combined form to extract the optimized parameter setting which can maximize or minimize an output parameter to a desired value. The combined objective considers all the output responses in together and finds the ranking of alternatives considered. The experimental data is processed for determining the weights to be assigned for individual output response and further subjected for multi objective optimization. The combined objective becomes a single value after processing the experimental data and it is termed as multi response performance index. Alternative with higher value of multi response performance index is considered as ranking top.

Principal Component Analysis

The weights of responses need to be calculated for understanding its importance in combined objective optimization. The current study utilizes principal component analysis which actually reduces the dimension of a dataset by calculating eigen values for the principal components. The principal component having the major contribution is considered and after calculating eigen vectors the principal component with highest contribution is considered for evaluating the weights of response. In current study first principal component is found to have maximum contribution of 66.4% and contribution of other principal components is shown in Table 10. After calculating eigen vectors for principal components the square of eigen vector of principal component with higher contribution (PC1) is considered as the response weight. Hence in current study the weight for change in length is 31%, 48% for change in width and 21% for change in thickness. Tables 10 and 11 shows the eigen values and eigen vectors for principal components.

Table 10. Eigen values and proportions for Principal Components

Principal Component	Eigen Value	Proportion
First	1.9928	0.664
Second	0.9409	0.314
Third	0.0663	0.022

Table 11. Eigen vectors for Principal Components and contributions

Output Parameter	PC1	PC2	PC3	Weightage
ΔL (mm)	0.555	-0.623	0.551	0.31
ΔW (mm)	0.696	-0.014	-0.718	0.48
ΔT (mm)	-0.455	-0.782	-0.426	0.21

TOPSIS

TOPSIS (Technique Order Preference Similar to Ideal Solution) is one of MCDM methods considers both the distance of each alternative from the positive ideal and the distance of each alternative from the negative ideal point. In other words, the best alternative should have the shortest distance from the positive ideal solution (PIS) and the longest distance from the negative ideal.

In this study there are 3 criteria's and 18 alternatives that are ranked based on TOPSIS method. The following table describes the criteria.

The Steps of the TOPSIS Method:

STEP 1: Normalize the decision-matrix.

The following formula can be used to normalize.

$$r_{ij}(\mathrm{x}) = \frac{x_{ij}}{\sqrt{\sum_{i=1}^{m} x_{ij}^2}} \qquad i = 1, \dots, m \;\; ; j = 1, \dots \;\; , n \tag{1}$$

The following Table 12 shows the normalized matrix.

STEP 2: Calculate the weighted normalized decision matrix.

According to the following formula, the normalized matrix is multiplied by the weight of the criteria.

$$v_{ij}(\mathrm{x}) = w_j r_{ij}(x) \qquad i = 1, \dots, m \;\; ; j = 1, \dots \;\; , n \tag{2}$$

The following Table 12 shows the weighted normalized decision matrix.

Table 12. Normalized and Weighted Normalized Values PCA-TOPSIS

Trial No	A	B (mm)	C (%)	D (°)	E	Normalized			Weighted Normalized		
						ΔL (mm)	ΔW (mm)	ΔT (mm)	ΔL (mm)	ΔW (mm)	ΔT (mm)
1	1	1	1	1	1	0.1096	0.0343	0.0281	0.0338	0.0166	0.0058
2	1	1	2	2	2	0.2001	0.2105	0.0094	0.0616	0.1020	0.0019
3	1	1	3	3	3	0.2144	0.2741	0.0094	0.0660	0.1328	0.0019
4	1	2	1	1	2	0.3192	0.3622	0.0047	0.0983	0.1755	0.0010
5	1	2	2	2	3	0.2954	0.3084	0.0938	0.0910	0.1494	0.0194
6	1	2	3	3	1	0.3239	0.4503	0.0235	0.0998	0.2181	0.0049
7	1	3	1	2	1	0.2048	0.2398	0.0047	0.0631	0.1162	0.0010
8	1	3	2	3	2	0.4240	0.4846	0.0047	0.1306	0.2347	0.0010
9	1	3	3	1	3	0.3239	0.3867	0.0844	0.0998	0.1873	0.0175
10	2	1	1	3	3	0.0238	0.0979	0.1642	0.0073	0.0474	0.0340
11	2	1	2	1	1	0.0381	0.1126	0.0891	0.0117	0.0545	0.0185
12	2	1	3	2	2	0.1286	0.1224	0.1876	0.0396	0.0593	0.0388
13	2	2	1	2	3	0.2096	0.0881	0.3893	0.0646	0.0427	0.0806
14	2	2	2	3	1	0.1191	0.0832	0.2252	0.0367	0.0403	0.0466
15	2	2	3	1	2	0.3144	0.1322	0.4081	0.0968	0.0640	0.0845
16	2	3	1	3	2	0.1858	0.0636	0.3330	0.0572	0.0308	0.0689
17	2	3	2	1	3	0.2382	0.1615	0.2721	0.0734	0.0782	0.0563
18	2	3	3	2	1	0.2906	0.1175	0.3940	0.0895	0.0569	0.0816

STEP 3: Determine the positive ideal and negative ideal solutions.

The aim of the TOPSIS method is to calculate the degree of distance of each alternative from positive and negative ideals. Therefore, in this step, the positive and negative ideal solutions are determined according to the following formulas.

$$A^+ = (v_1^+, v_2^+, \dots, v_n^+) \quad (3)$$

$$A^- = (v_1^-, v_2^-, \dots, v_n^{-+}) \quad (4)$$

So that

$$v_j^+ = \left\{\left(max\ v_{ij}(x)\middle|\ j\epsilon j_1\right), \left(min\ v_{ij}(x)\middle|\ j\epsilon j_2\right)\right\}\ i = 1, \dots, m \quad (5)$$

$$v_j^- = \left\{\left(min\ v_{ij}(x)\middle|\ j\epsilon j_1\right), \left(max\ v_{ij}(x)\middle|\ j\epsilon j_2\right)\right\}\ i = 1, \dots, m \quad (6)$$

where j_1 and j_2 denote the negative and positive criteria, respectively.

The following table shows both positive and negative ideal values.

STEP 4: Distance from the positive and negative ideal solutions

TOPSIS method ranks each alternative based on the relative closeness degree to the positive ideal and distance from the negative ideal. Therefore, in this step, the calculation of the distances between each alternative and the positive and negative ideal solution is obtained by using the following formulas.

$$d_i^+ = \sqrt{\sum_{j=1}^{n}[v_{ij}(x) - v_j^+(x)]^2} \quad , \quad i = 1, \dots, m \tag{7}$$

$$d_i^- = \sqrt{\sum_{j=1}^{n}[v_{ij}(x) - v_j^-(x)]^2} \quad , \quad i = 1, \dots, m \tag{8}$$

The following Table 13 shows the distance to the positive and negative ideal solutions.

STEP 5: Calculate the relative closeness degree of alternatives to the ideal solution

In this step, the relative closeness degree of each alternative to the ideal solution is obtained by the following formula. If the relative closeness degree has value near to 1, it means that the alternative has shorter distance from the positive ideal solution and longer distance from the negative ideal solution.

$$C_i = \frac{d_i^-}{(d_i^+ + d_i^-)} \quad , \quad i = 1, \dots, m \tag{9}$$

The following table shows the relative closeness degree of each alternative to the ideal solution and its ranking. Table 13 shows the positive ideal, negative ideal solutions and Closeness coefficient values with ranking of alternatives.

Table 13. Positive Ideal, Negative Ideal Solution and Closeness Coefficient Values

Trial No	Si+	Si-	Cci	Rank
1	0.0269	0.2513	0.9034	1
2	0.1012	0.1709	0.6281	8
3	0.1302	0.1462	0.5290	13
4	0.1831	0.1074	0.3697	15
5	0.1580	0.1144	0.4200	14
6	0.2218	0.0870	0.2817	17
7	0.1141	0.1600	0.5836	11
8	0.2505	0.0835	0.2500	18
9	0.1948	0.0877	0.3104	16
10	0.0452	0.2298	0.8358	3
11	0.0420	0.2257	0.8431	2
12	0.0656	0.2028	0.7557	5
13	0.1015	0.2031	0.6669	7
14	0.0592	0.2192	0.7873	4
15	0.1313	0.1740	0.5700	12
16	0.0855	0.2173	0.7176	6
17	0.1059	0.1690	0.6146	9
18	0.1220	0.1825	0.5995	10

Table 14 ANOVA Results for PCA-TOPSIS Closeness Coefficient Values

Source	DF	Adj SS	Adj MS	F-Value	P-Value	Contribution %
A	1	0.175566	0.175566	25.28	0.001	30.01
B	2	0.219531	0.109766	15.81	0.002	37.52
C	2	0.081222	0.040611	5.85	0.027	13.88
D	2	0.004374	0.002187	0.31	0.738	0.75
F	2	0.048786	0.024393	3.51	0.08	8.34
Error	8	0.055555	0.006944	---	---	9.50
Total	17	0.585035	---	---	---	100.00

Table 15. Model Summary for PCA-TOPSIS Closeness Coefficient Values

S	R-sq	R-sq (adj)	R-sq (pred)
0.08333	90.50%	79.82%	51.93%

The ranking of PCA-TOPSIS ranks the 1st alternative with parameter combination A1B1C1D1E1 as the best one and 8th alternative A1B3C2D3E2 as the worst alternative for the combined objectives. The ranking of alternatives follows the order 1>11>10>14>12>16>13>2>17>18>7>15>3>5>4>9>6>8.The closeness coefficient values are further analyzed using ANOVA with a confidence interval of 95% with p-value less than 0.05 is considered as significant. From ANOVA results shown in Table 14, the input parameters layer thickness, build orientation and infill density are found to be significant. Layer thickness has a crucial contribution of 37.52%, build orientation has 30.01% contribution and infill density has 13.88% contribution. The error percentage is 9.50 which is under acceptable range. The model summary values indicated in Table 15 ensures that R-squared value with 90.50% is a good sign that the changes in output response can be explained by independent variable with an accuracy of 90.50.

Table 16. Response Table for PCA-TOPSIS Closeness Coefficient Values

Level	A	B	C	D	E
1	-6.693	-2.633	-3.701	-4.933	-4.001
2	-3.294	-6.125	-5.043	-4.481	-5.641
3	---	-6.223	-6.237	-5.567	-5.339
Delta	3.398	3.590	2.537	1.087	1.64
Rank	2	1	3	5	4

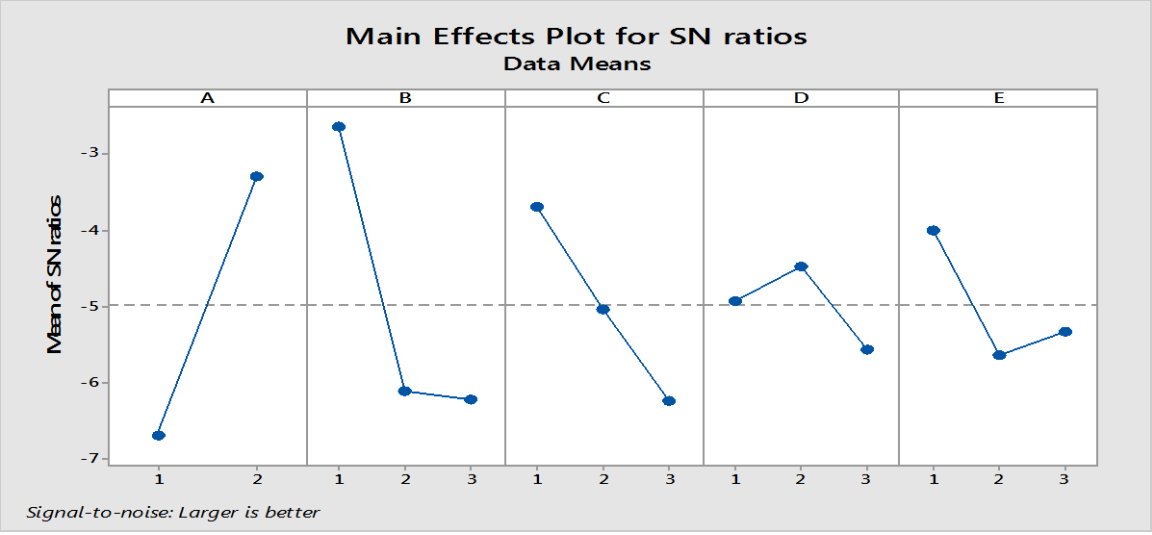

Figure 5. Main Effect Plot for PCA-TOPSIS Closeness Coefficient Values

The closeness coefficient values are further analyzed using signal to noise method with higher the better characteristic using Minitab 17.0.The main effect plot shown in Figure 5 recommends the combination A2B1C1D2E1 (On edge Orientation , 0.1 mm layer thickness , 50% infill density , 45º raster angle and cubic infill pattern) for improving the closeness coefficient value. The response table rankings highlighted in Table 16 indicates that layer thickness is the top most influencing parameter followed by build orientation, infill density, infill pattern and raster angle. The rankings of response table are in good accordance with ANOVA results.

Shanon's Entropy Method

Entropy method was introduced in the year 1948 by Shanon which normalizes the experimental data through decision matrix and transforms them in to corresponding project outcome. The project outcomes evaluated are utilized for computing the entropy measure and to obtain the objective weights which can provide the weight of output responses. The weight value calculated shows that changes in thickness has maximum weight of 60%, followed by changes in width by 25% and 15% weightage for changes in length. Table17 shows the weights obtained for output responses as per entropy method.

Table 17. Weights of output Responses – Entropy

Output Parameter	Weightage
ΔL (mm)	0.15
ΔW (mm)	0.25
ΔT (mm)	0.60

CoCoSo

Combined Compromise Solution (CoCoSo) method is an integrated approach based on simple additive weighting and weighted product models. Its procedural steps are enumerated as below.

STEP 1: Development of the initial decision matrix as shown in equation 10. The corresponding decision matrix is first formulated considering m alternatives (number of experimental trials) and n criteria (number of responses).

$$X = \begin{bmatrix} x_{11} & x_{12} & \dots & x_{1n} \\ x_{21} & x_{22} & \dots & x_{2n} \\ x_{m1} & x_{m2} & \dots & x_{mn} \end{bmatrix} \quad (10)$$

STEP 2: Normalization of the decision matrix

Depending on the type of the criterion considered, the initial decision matrix is now normalized employing the following equations 11 and 12.

The current study focus on reducing the dimensional inaccuracy of the part printed. Hence all the four output responses fall under the category of lower the better criterion.

For beneficial (higher-the-better) criterion:

$$\boldsymbol{n_{ij}} = \frac{\boldsymbol{x_{ij} - max\, x_{ij}}}{\boldsymbol{max\, x_{ij} - min\, x_{ij}}} \quad (11)$$

For non-beneficial (lower-the-better) criterion:

$$n_{ij} = \frac{max\, x_{ij} - x_{ij}}{max\, x_{ij} - min\, x_{ij}} \quad (12)$$

where n_{ij} is the normalized value of x_{ij}.

STEP 3: Calculation of the power of weighted (P_i) and sum of weighted (S_i) comparability sequence scores using equation 13 and 14. The power of weighted comparability and sum of weighted comparability sequence scores are computed for each of the alternatives.

$$P_i = \sum_{j=1}^{n} (n_{ij})^{w_{ij}} \quad (13)$$

$$S_i = \sum_{j=1}^{n} (w_j * n_{ij}) \quad (14)$$

STEP 4: Estimation of the appraisal scores the appraisal scores of each alternative can now be calculated using the following three aggregation strategies mentioned in equation 15, 16 and 17.

$$a_{ia} = \frac{(P_i + S_i)}{\sum_{i=1}^{n}(P_i + S_i)} \quad (15)$$

$$a_{ib} = \frac{P_i}{min\ P_i} + \frac{S_i}{min\ S_i} \quad (16)$$

$$a_{ic} = \frac{\lambda * P_i + (1-\lambda) * S_i}{\lambda * max\ P_i + (1-\lambda) * max\ S_i} \quad (17)$$

The current study considers λ value as 0.5 ($0 < \lambda < 1$)

STEP 5: Calculation of the final appraisal score (A_i) using equation 18.

$$A_i = (a_{ia} * a_{ib} * a_{ic})^{\frac{1}{3}} + \frac{1}{3}\ (a_{ia} * a_{ib} * a_{ic}) \quad (18)$$

Table 18 shows the normalized and weighted normalized values.

Table 18. Normalized and Weighted Normalized Values Entropy - CoCoSo

Trial No.	A	B (mm)	C (%)	D (°)	E	Normalized			Weighted Normalized		
						ΔL (mm)	ΔW (mm)	ΔT (mm)	ΔL (mm)	ΔW (mm)	ΔT (mm)
1	1	1	1	1	1	0.7857	1.0698	0.9419	0.1179	0.2674	0.5651
2	1	1	2	2	2	0.5595	0.6512	0.9884	0.0839	0.1628	0.5930
3	1	1	3	3	3	0.5238	0.5000	0.9884	0.0786	0.1250	0.5930
4	1	2	1	1	2	0.2619	0.2907	1.0000	0.0393	0.0727	0.6000
5	1	2	2	2	3	0.3214	0.4186	0.7791	0.0482	0.1047	0.4674
6	1	2	3	3	1	0.2500	0.0814	0.9535	0.0375	0.0203	0.5721
7	1	3	1	2	1	0.5476	0.5814	1.0000	0.0821	0.1453	0.6000
8	1	3	2	3	2	0.0000	0.0000	1.0000	0.0000	0.0000	0.6000
9	1	3	3	1	3	0.2500	0.2326	0.8023	0.0375	0.0581	0.4814
10	2	1	1	3	3	1.0000	0.9186	0.6047	0.1500	0.2297	0.3628
11	2	1	2	1	1	0.9643	0.8837	0.7907	0.1446	0.2209	0.4744
12	2	1	3	2	2	0.7381	0.8605	0.5465	0.1107	0.2151	0.3279
13	2	2	1	2	3	0.5357	0.9419	0.0465	0.0804	0.2355	0.0279
14	2	2	2	3	1	0.7619	0.9535	0.4535	0.1143	0.2384	0.2721
15	2	2	3	1	2	0.2738	0.8372	0.0000	0.0411	0.2093	0.0000
16	2	3	1	3	2	0.5952	1.0000	0.1860	0.0893	0.2500	0.1116
17	2	3	2	1	3	0.4643	0.7674	0.3372	0.0696	0.1919	0.2023
18	2	3	3	2	1	0.3333	0.8721	0.0349	0.0500	0.2180	0.0209

Table 19. Compatibility Sequence Score and Appraisal Scores for the Alternatives

Trial No	Si	Pi	a_{ia}	a_{ib}	a_{ic}	A_i	Rank
1	0.9504	2.1548	0.0725	6.7236	1.0000	3.3617	1
2	0.8397	2.0557	0.0676	6.1469	0.9324	3.0899	3
3	0.7966	2.0083	0.0655	5.9102	0.9033	2.9771	5
4	0.7120	1.8706	0.0603	5.3851	0.8317	2.7207	7
5	0.6203	1.8370	0.0574	4.9733	0.7913	2.5333	10
6	0.6299	1.7041	0.0545	4.8312	0.7516	2.4463	11
7	0.8275	2.0408	0.0670	6.0778	0.9237	3.0568	4
8	0.6000	0.7360	0.0312	3.3964	0.4303	1.6340	16
9	0.5770	1.7470	0.0543	4.6783	0.7484	2.3869	12
10	0.7424	1.9888	0.0638	5.6675	0.8796	2.8667	6
11	0.8400	2.0731	0.0680	6.1716	0.9381	3.1040	2
12	0.6537	1.9121	0.0599	5.2089	0.8263	2.6508	8
13	0.3437	1.4985	0.0430	3.4088	0.5933	1.7816	15
14	0.6248	1.8790	0.0585	5.0481	0.8063	2.5739	9
15	0.2504	1.2959	0.0361	2.7606	0.4980	1.4585	18
16	0.4509	1.6714	0.0496	4.0719	0.6835	2.1057	14
17	0.4638	1.7158	0.0509	4.1837	0.7019	2.1631	13
18	0.2890	1.4196	0.0399	3.0829	0.5502	1.6233	17

Table 19 shows the various scores obtained and their rankings. The higher value of appraisal score is considered as the best for attaining the combined objectives and the lowest value is considered as the worst alternative. Entropy-CoCoSo recommends the combination A1B1C1D1E1 (1st Alternative) as the top alternative and A2B2C3D1E2 (15th Alternative) as worst alternative. The ranking of alternative follows the order 1>11>2>7>3>10>4>12>14>5>6>9>17>16>13>8>18>15.ANOVA results in Table 20 indicates that 46.33% contribution goes to layer thickness , 14.93 % of contribution for build orientation and infill pattern with 9.44%.The error percentage of ANOVA is resulted with 20.21%.

Table 20. ANOVA Results for Entropy – CoCoSo Appraisal Score

Source	DF	Adj SS	Adj MS	F-Value	P-Value	Contribution %
A	1	0.8359	0.8359	5.91	0.041	14.93
B	2	2.5933	1.2966	9.17	0.009	46.33
C	2	0.4765	0.2382	1.68	0.245	8.51
D	2	0.0321	0.0160	0.11	0.894	0.57
F	2	0.5281	0.2640	1.87	0.216	9.44
Error	8	1.1315	0.1414	---	---	20.21
Total	17	5.5972	---	---	---	100.00

Table 21. Model Summary for Entropy – CoCoSo Appraisal Score

S	R-sq	R-sq (adj)	R-sq (pred)
0.376073	79.78%	57.04%	0.00%

Table 22. Response Table for Entropy – CoCoSo Appraisal Score

Level	A	B	C	D	E
1	8.430	9.543	8.260	7.767	8.377
2	6.815	6.841	7.815	7.545	6.829
3	---	6.484	6.793	7.556	7.662
Delta	1.615	3.059	1.468	0.222	1.549
Rank	2	1	4	5	3

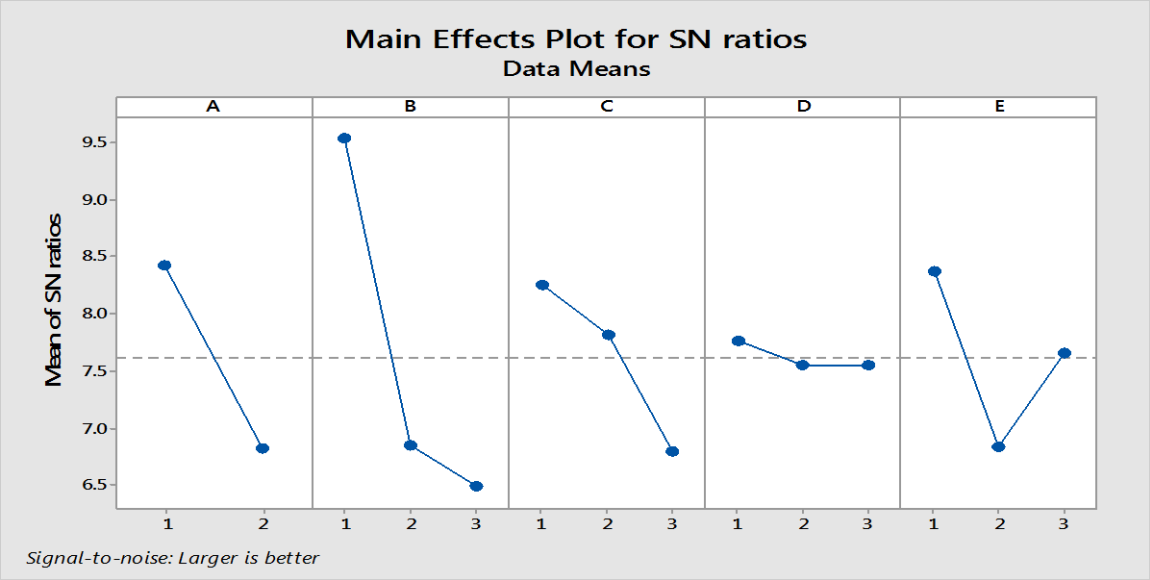

Figure 6. Main Effect Plot for Entropy - CoCoSo Appraisal Score

R-squared value of 79.78% indicates that the changes in output responses can be explained by independent variable with an accuracy of 79.78%.Model summary is shown in Table 21.The main effect plot produced by analyzing the Entropy-CoCoSo appraisal scores with higher the better, signal to noise ratio method recommends the combination A1B1C1D1E1 (Flat Orientation, 0.1 mm layer thickness, 50% infill density, 0º raster angle and cubic infill pattern) as shown in Figure 6. The response table shown in Table 22 ranks layer thickness as top subsequently followed by build orientation, infill pattern, infill density and raster angle. The rankings of response table are in good accordance with ANOVA results.

Confirmation Trials

The combination of parameters obtained from both the methods have been considered for confirmation trials in order to examine their potential in obtaining reduced dimensional deviations. The optimal parameter combination is found to have similarity in the levels of layer thickness, infill density and infill pattern. But in case of build orientation and raster angle different factor levels have been recommended.

Table 23. Comparison Table for Optimal Parameter Settings

S. No	Method	Optimal Parameter Combination	A	B (mm)	C (%)	D (°)	E	ΔL (mm)	ΔW (mm)	ΔT (mm)
1	Entropy - CoCoSo	A1B1C1D1E1	Flat	0.1mm	50%	0	Cubic	0.11	0.12	-0.09
2	PCA-TOPSIS	A2B1C1D2E1	On edge	0.1mm	50%	45	Cubic	0.40	-0.27	0.21

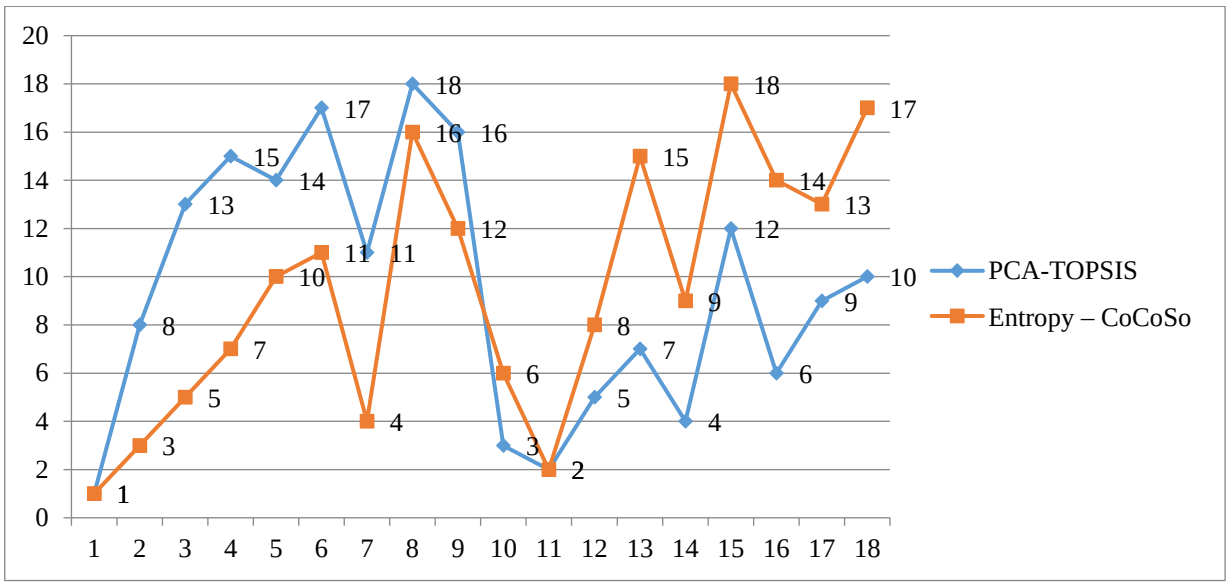

Figure 7. Comparison of Alternative Ranking's PCA-TOPSIS and Entropy – CoCoSo

The comparison of rankings obtained for the multi response performance index (Closeness Coefficient Values and Final Appraisal scores) shows that the ranking of top alternative is similar for both the methods adopted and other rankings are varied. The rankings obtained from both the methods have a correlation of 43.46%. Figure 7 shows the plot between the rankings of MRPI values. The confirmation trials carried out has revealed that lower deviations are resulted from Entropy – CoCoSo method. Table 23 shows the Comparison Table for Optimal Parameter Settings

Machine Learning

Machine learning techniques enable systems to learn from experience to make wise predictions. Decision trees are supervised machine learning techniques which can be used for both classification and regression problems. It has a hierarchical tree structure which consists of root node, branch nodes, internal nodes and leaf nodes. The current study analyzes the experimental data using three different supervised machine learning algorithms such as decision tree, random forest and Naïve Bayes. The final appraisal scores obtained from Entropy-CoCoSo has been classified in to class 1 and class 2 instances based upon average value 2.4741 from the dataset. Class 1 represents appraisal score values ranging from average value (0 – 2.4741) and Class 2 is assigned for above average values (2.4741 – 3.3617). Based upon the classification out of 18 instances, 8 instances are classified as class 1 and 10 instances are classified as class 2. The dataset has been saved in .CSV format and inputted with Orange open source machine learning software with a training-testing split ratio of 75:25. Table 24 shows the dataset used for training with classes applied.

Table 24. Dataset with Class Labels for Training and Testing using Classification Algorithms

Trial No	A	B (mm)	C (%)	D (º)	E	Ai	Class Label
1	1	1	1	1	1	3.3617	Class 2
2	1	1	2	2	2	3.0899	Class 2
3	1	1	3	3	3	2.9771	Class 2
4	1	2	1	1	2	2.7207	Class 2
5	1	2	2	2	3	2.5333	Class 2
6	1	2	3	3	1	2.4463	Class 1
7	1	3	1	2	1	3.0568	Class 2
8	1	3	2	3	2	1.6340	Class 1
9	1	3	3	1	3	2.3869	Class 1
10	2	1	1	3	3	2.8667	Class 2
11	2	1	2	1	1	3.1040	Class 2
12	2	1	3	2	2	2.6508	Class 2
13	2	2	1	2	3	1.7816	Class 1
14	2	2	2	3	1	2.5739	Class 2
15	2	2	3	1	2	1.4585	Class 1
16	2	3	1	3	2	2.1057	Class 1
17	2	3	2	1	3	2.1631	Class 1
18	2	3	3	2	1	1.6233	Class 1

Table 25. Comparison of Evaluation Metrics – Classification Algorithms

Method	AUC	CA	F1	Precision	Recall
Tree	0.938	0.889	0.889	0.889	0.889
Random Forest	0.950	0.778	0.778	0.778	0.778
Naïve Bayes	0.994	0.994	0.994	0.949	0.944

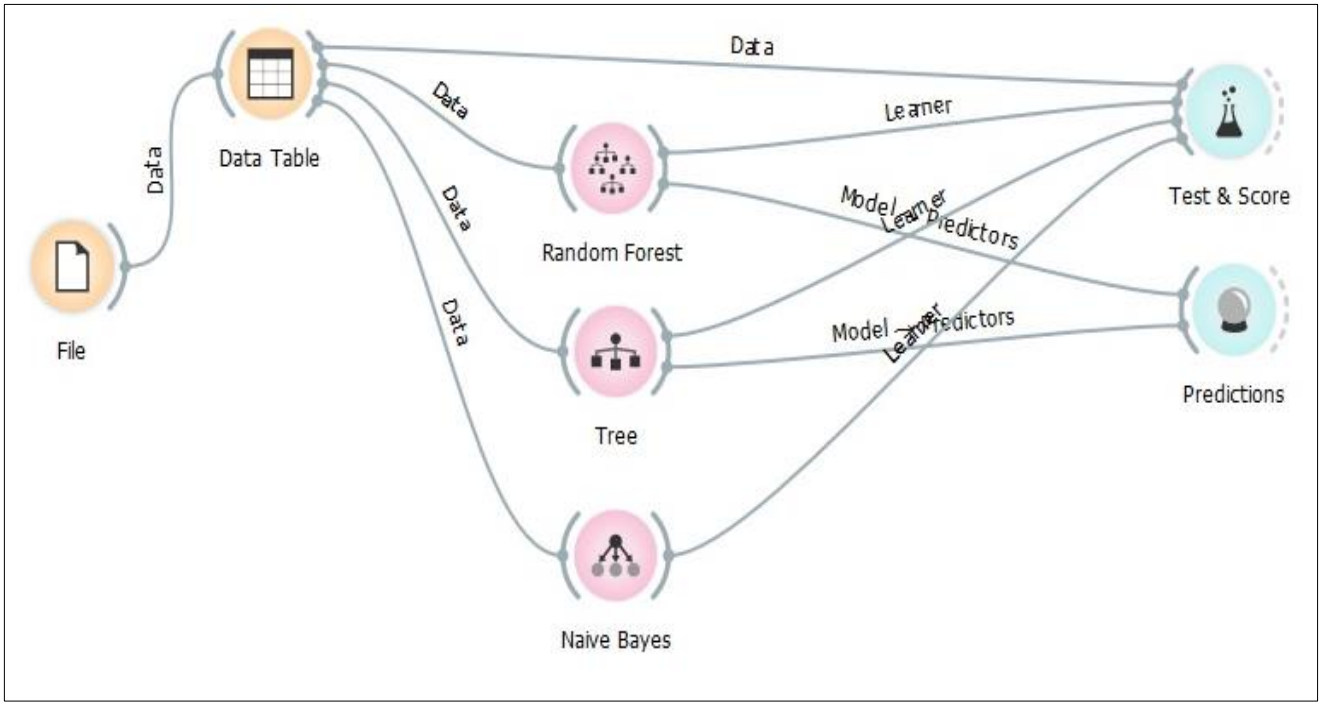

Figure 8. Schematic representation of Machine Learning Workflow

Table 25 shows the values of evaluation metrics for dataset trained using classification algorithms. From the results, it can be observed that the performance of Naïve Bayes algorithm is superior to other models considered. It has resulted with a maximum accuracy of 99.4% followed by decision tree method with 88.9% and 77.8% accuracy is attained by random forest method. Naïve Bayes method can predict the targeted output response values with low error percentage. Figure 8 shows the schematic representation of machine learning workflow.

4. Conclusions

The current study has considered nylon filament reinforced with 20% carbon fiber to investigate the effect of five different input factors such as build orientation, layer thickness, infill density, raster angle and infill pattern. The geometric devotions observed using combined approaches such as Entropy-CoCoSo and PCA-TOPSIS. The multi response performance index values further trained using classification based machine learning algorithms. The major findings are summarized below.

The deviations in sample length, width and thickness has been tabulated for analysis and it is observed that only positive deviations have occurred in the length dimension, both positive and negative deviations are resulted in width and thickness dimensions.

ANOVA has been employed to find the significant parameter in an individual manner and it has been understood layer thickness is dominant for deviations in length with 46.96% contribution. Build orientation has superior dominance than other parameters over width and thickness deviations with 52.53 and 70.02% contribution.

Main effect plot has recommended different combinations for reducing the deviations separately, where A2B1C1D3E1 is recommended for reducing deviations in length, A2B1C1D1E1 is recommended for reducing deviations in width and A2B1C1D3E2 is suggested for reducing deviations in thickness. The significance recommended by both ANOVA and Response table are similar.

The weights of output responses have been evaluated using entropy and principal component analysis methods. Entropy method has recommended 15% weigh for change in length, 25% weight for change in width and 60% weight for change in thickness. But Principal component method has recommended 31% weigh for change in length, 48% weight for change in width and 21% weight for change in thickness.

The optimal parameter combination suggested by Entropy-CoCoSo method A1B1C1D1E1 has resulted in lowest geometric deviation such as $\Delta L = 0.11$ mm, $\Delta W = 0.12$ mm and $\Delta T = -0.09$ mm when comparing the optimal parameter combination recommended by PCA-TOPSIS method A2B1C1D2E1, where $\Delta L = 0.40$ mm, $\Delta W = -0.27$ mm and $\Delta T = -0.21$ mm. Only the top ranked alternative is similar from both the methods adopted.

Layer thickness is the top ranked parameter affecting the multi response performance index values towards combined objectives with maximum contribution of 46.33 % and subsequently followed by part orientation.

The multi response performance index values of Entropy-CoCoSo method has been trained and tested using decision tree, random forest and Naïve Bayes algorithm. Naïve Bayes algorithm out-performed other classification algorithm with 99.4% classification accuracy.

Regression based ML algorithms may be employed to analyse the experimental outcome to identify the optimal parameter settings which reduces dimensional error in all three directions.

Confirmation trails conducted have shown that the optimal parameter combinations obtained through Entropy-CoCoSo method has low dimensional error and they are much closer to the tolerance limit.

Post processing of the printed samples may further reduce the deviation.

References

1.E. MOLERO, J. J. FERNÁNDEZ, O. RODRÍGUEZ-ALABANDA, G. GUERRERO-VACA, P. E. ROMERO, "Use of data mining techniques for the prediction of surface roughness of printed parts in polylactic acid (PLA) by fused deposition modeling (FDM): A practical application in frame glasses

manufacturing," *Polymers (Basel).*, vol. 12, no. 4, 2020, doi: 10.3390/POLYM12040840.
2.X. ZHANG, W. FAN, T. LIU, "Fused deposition modeling 3D printing of polyamide-based composites and its applications," *Compos. Commun.*, vol. 21, no. June, 2020, doi: 10.1016/j.coco.2020.100413.
3.P. K. PENUMAKALA, J. SANTO, A. THOMAS, "A critical review on the fused deposition modeling of thermoplastic polymer composites," vol. 201, no. August, 2020.
4.K. MUHAMEDAGIC *et al.*, "Effect of Process Parameters on Tensile Strength of FDM Printed Carbon Fiber Reinforced Polyamide Parts," *Appl. Sci.*, vol. 12, no. 12, 2022, doi: 10.3390/app12126028.
5.J. PARK, J. JEON, J. KOAK, S. KIM, "Dimensional accuracy and surface characteristics of 3D-printed dental casts," pp. 1–11.
6.R. MENDRICKY, D. FRIS, "Analysis of the accuracy and the surface roughness of fdm/fff technology and optimisation of process parameters," *Teh. Vjesn.*, vol. 27, no. 4, pp. 1166–1173, 2020, doi: 10.17559/TV-20190320142210.
7.P. SHARMA, H. VAID, R. VAJPEYI, P. SHUBHAM, K. M. AGARWAL, D. BHATIA, "Predicting the dimensional variation of geometries produced through FDM 3D printing employing supervised machine learning," *Sensors Int.*, vol. 3, no. July, p. 100194, 2022, doi: 10.1016/j.sintl.2022.100194.
8.P. J. NUÑEZ, A. RIVAS, E. GARCÍA-PLAZA, E. BEAMUD, A. SANZ-LOBERA, "Dimensional and surface texture characterization in Fused Deposition Modelling (FDM) with ABS plus," *Procedia Eng.*, vol. 132, pp. 856–863, 2015, doi: 10.1016/j.proeng.2015.12.570.
9.A. NORIEGA, D. BLANCO, B. J. ALVAREZ, A. GARCIA, "Dimensional accuracy improvement of FDM square cross-section parts using artificial neural networks and an optimization algorithm," 2013, doi: 10.1007/s00170-013-5196-2.
10.R. SINGH, A. TRIVEDI, "Experimental Investigations for Surface Roughness and Dimensional Accuracy of FDM Components with Barrel Finishing," 2017, doi: 10.1007/s40010-017-0367-4.
11.N. DECKER, A. YEE, "A simplified benchmarking model for the assessment of dimensional accuracy in FDM processes," vol. 5, no. 2, pp. 145–154, 2015.
12.R. SINGH, J. SINGH, S. SINGH, "Investigation for dimensional accuracy of AMC prepared by FDM assisted investment casting using nylon-6 waste based reinforced filament Fabrication of IC Patterns," vol. 78, pp. 253–259, 2016.
13.J. SINGH, C. RUPINDER, "Enhancing dimensional accuracy of FDM based biomedical implant replicas by statistically controlled vapor smoothing process," pp. 105–113, 2016, doi: 10.1007/s40964-016-0009-4.
14.P. PSO, B. EAGLE, S. ALGORITHMS, "Analysis and Optimization of Dimensional Accuracy and Porosity of High Impact Polystyrene Material Printed by FDM," pp. 1–20, 2021.
15.S. L. MESSIMER, T. R. PEREIRA, A. E. PATTERSON, M. LUBNA, "Full-Density Fused Deposition Modeling Dimensional Error as a Function of Raster Angle and Build Orientation : Large Dataset for Eleven Materials", doi: 10.3390/jmmp3010006.
16.J. S. CHOHAN, R. SINGH, K. S. BOPARAI, R. PENNA, F. FRATERNALI, "SC," 2017, doi: 10.1016/j.compositesb.2017.02.045.This.
17.O. A. MOHAMED, S. H. MASOOD, J. L. BHOWMIK, "Modeling, analysis, and optimization of dimensional accuracy of FDM-fabricated parts using definitive screening design and deep learning feedforward artificial neural network," *Adv. Manuf.*, vol. 9, no. 1, pp. 115–129, 2021, doi: 10.1007/s40436-020-00336-9.
18.P. K. KOPPARTHI, V. R. KUNDAVARAPU, "Modeling and multi response optimization of mechanical properties for E-glass / polyester composite using Taguchi-grey relational analysis," 2020, doi: 10.1177/0954408920962592.
19.S. SUDHAGAR, M. SAKTHIVEL, P. J. MATHEW, S. A. A. DANIEL, "A multi criteria decision making approach for process improvement in friction stir welding of aluminium alloy," *Meas. J. Int. Meas. Confed.*, vol. 108, pp. 1–8, 2017, doi: 10.1016/j.measurement.2017.05.023.

20.P. PATIL, D. SINGH, S. J. RAYKAR, J. BHAMU, "Multi-objective optimization of process parameters of Fused Deposition Modeling (FDM) for printing Polylactic Acid (PLA) polymer components," *Mater. Today Proc.*, vol. 45, pp. 4880–4885, 2021, doi: 10.1016/j.matpr.2021.01.353.
21.M. S. SAPRE, A. V JATTI, N. K. KHEDKAR, V. S. JATTI, "Mechanical Properties of 3D-Printed Components Using Fused Deposition Modeling : Optimization Using the Desirability Approach and Machine Learning Regressor," 2022.
22.J. M. BARRIOS, P. E. ROMERO, "Decision tree methods for predicting surface roughness in fused deposition modeling parts," *Materials (Basel).*, vol. 12, no. 16, 2019, doi: 10.3390/ma12162574.
23.P. MISHRA, S. SOOD, V. BHARADWAJ, A. AGGARWAL, P. KHANNA, "Parametric Modeling and Optimization of Dimensional Error and Surface Roughness of Fused Deposition Modeling Printed Polyethylene Terephthalate Glycol Parts," Polymers (Basel)., vol. 15, no. 3, 2023, doi: 10.3390/polym15030546.
24.NAGENDRA KUMAR MAURYA, VIKAS RASTOGI, PUSHPENDRA SINGH, Investigation of dimensional accuracy and international tolerance grades of 3D printed polycarbonate parts, Materials Today: Proceedings, Volume 25, Part 4, 2020, Pages 537-543, ISSN 2214-7853, https://doi.org/10.1016/j.matpr.2019.06.007.
25.K. E. ASLANI, K. KITSAKIS, J. D. KECHAGIAS, N. M. VAXEVANIDIS, D. E. MANOLAKOS, "On the application of grey Taguchi method for benchmarking the dimensional accuracy of the PLA fused filament fabrication process," SN Appl. Sci., vol. 2, no. 6, 2020, doi: 10.1007/s42452-020-2823-z.

Manuscript received: 12.06.2023